JOURNAL OF MATERIALS SCIENCE 26 (1991) 3202–3208

Characterization of the SiC and TiN whisker microstructure

J. ZHU*, X. G. NING‡, H. G. XU*, K. Y. HU‡, W. CAO‡, H. Q. YE‡
*Central Iron and Steel Research Institute, Beijing 100081, People's Republic of China
‡Laboratory of Atomic Imaging of Solids, Institute of Metal Research, Academia Sinica, Shenyang 110015, People's Republic of China

Five criteria for evaluating the whisker microstructure have been suggested, which include (1) proportion of "perfect" single crystals, (2) morphology and growth direction, (3) length, diameter and ratio of L/D, (4) the bulk and surface chemistries, (5) defects and their distribution. Three sets of commercially available SiC whiskers made in two countries and the TiN whiskers were characterized in terms of the above criteria.

1. Introduction

SiC and TiN whiskers are of considerable interest as reinforcements for metal or ceramic matrix composites. SiC whisker-toughened aluminium has received much attention because of its attractive mechanical and thermal properties. The addition of SiC whiskers to toughen and strengthen mullite, zirconia and silicon nitride is being pursued for high-temperature applications. However, the use of TiN whiskers is rather limited. Owing to a good match of thermal properties between TiN whiskers and zirconia matrix, ZrO_2 composite material reinforced with TiN whiskers is a good candidate for advanced heat engines, cutting tools, and for other applications.

The basic mechanism of strengthening in the composite is the load transfer to the whiskers as pointed by Rice [1]. The mechanical properties of matrix and reinforcing whiskers will certainly affect the strength of composites. Recently, work has been performed in order to reveal that not only the mechanical properties of the whisker bulk, but also whisker microstructure may change the strength and the fracture toughness of composites. The strength and toughness of aluminium–20 vol % SiC whisker composites were improved with whisker length through increasing the pull-out length of the whisker [2]. The possibility of improved pull-out resistance using a twinned SiC whisker for reinforcement should not be overlooked [3]. Defects present in SiC whiskers may degrade the mechanical properties of the whiskers as well as the composites [4, 5]. The chemical and morphological properties of SiC whiskers would be expected to affect the processing and mechanical properties of the resulting composites [6].

Silicon carbide whiskers are currently available from several manufacturers. The characterization of whiskers reported by manufacturers normally involved phase composition, the diameter and length, Young's modulus, tensile strength, bulk compositions, etc., yet no thorough characterization of whisker microstructure has appeared in the literature. The intent of this work was to suggest five common factors for evaluating whisker microstructure, to present the main results for investigating SiC and TiN whiskers and thereby to understand better both the mechanisms of growth and the mechanical behaviour of the whiskers.

2. Experimental procedure

Three sets of SiC whiskers were used in this investigation. Two (labelled as C1 and C2) were made by the Institute of Metal Research, Academia Sinica and both were manufactured by a solid reaction method but treated by different procedures [7]. A third was a commercial product from Tokai Co., Japan (JTK). The TiN used was made by the Institute of Nuclear Energy Technology, Tsing Hua University, by chemical vapour deposition in the $TiCl_4$–N_2–H_2 system [8].

The phase composition of whiskers was examined by X-ray phase analysis. The morphology and microstructure of the whiskers were observed by analytical electron microscopy, JEOL 2000FX, and a high-resolution electron microscope, JEM 200CX, equipped with an ultra-high resolution pole-piece. Whiskers were easily dispersed; however, they seem to be rather thick for high-resolution imaging. Two kinds of composite reinforced by SiC whiskers with polymer and aluminum matrices, were obtained, and a cross-section of samples of whiskers was used in order to elucidate the transverse section shape and defect structures of the whiskers.

Bulk chemical composition analysis was carried out by energy dispersed spectrometry of X-ray microanalysis (EDS) in transmission electron microscopy

0022–2461/91 $03.00 + .12

(TEM) mode. Surface chemical composition analysis was performed in Riber Las 3000 and PEI 595 Auger electron spectrometers. The specimen used for surface analysis was prepared by impressing the whiskers into a soft indium plate. Thus the results obtained in surface analysis should be in the sense of statistics rather than an accurate measurement on a single whisker.

3. Results and discussion

The five criteria which are believed to be important for evaluating the whisker microstructure are

1. the phase composition and percentage of "perfect" single crystals;
2. the morphology, direction and plane of whisker growth;
3. the diameter, length and ratio between length and diameter;
4. the surface and bulk composition;
5. defect type and distribution.

The results for the SiC and TiN whiskers will be reported in turn.

3.1. Crystal structure and percentage of "perfect" single crystals

Phase identification was based on comparison with standard X-ray diffraction data cards. It was ascertained that only the β-SiC or TiN phases were present in the C1, C2, JTK and TiN whiskers obtained, respectively. TiN is an interstitial compound of NaCl-type structure with lattice constant $a_0 = 0.424$ nm. Fig. 1 shows a single TiN whisker with a straight rod shape and its selected-area electron diffraction patterns taken from different regions of the whisker. It can be seen that the electron diffraction patterns remain the same when moving along the whisker long-axis direction. The "perfect" whisker was defined as: (1) being a single crystal on the whole; (2) having a rather straight shape. About 50% TiN whiskers belong to the "perfect" group.

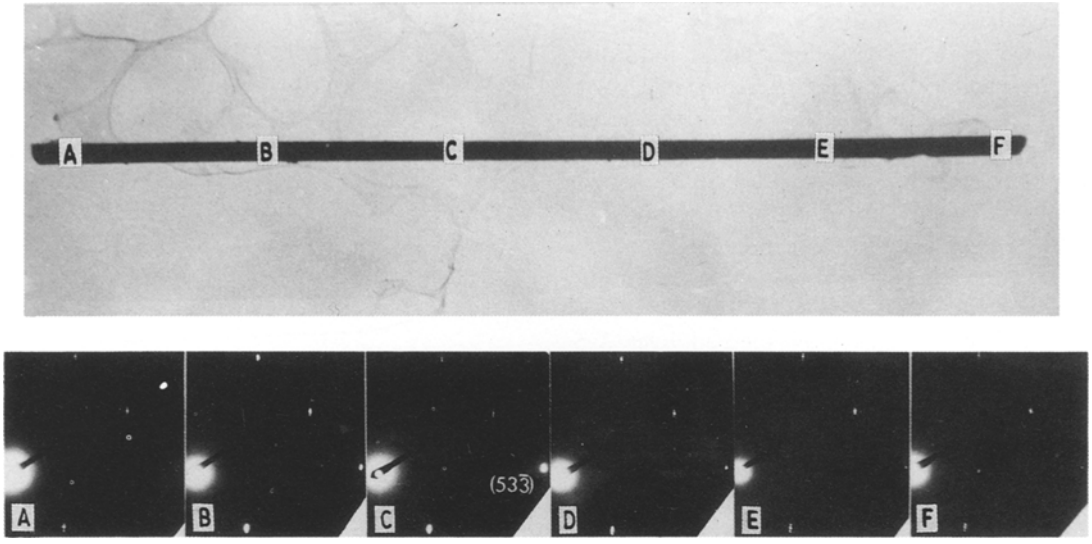

Figure 1 A straight TiN whisker with single-crystal structure on the whole, and with a straight shape.

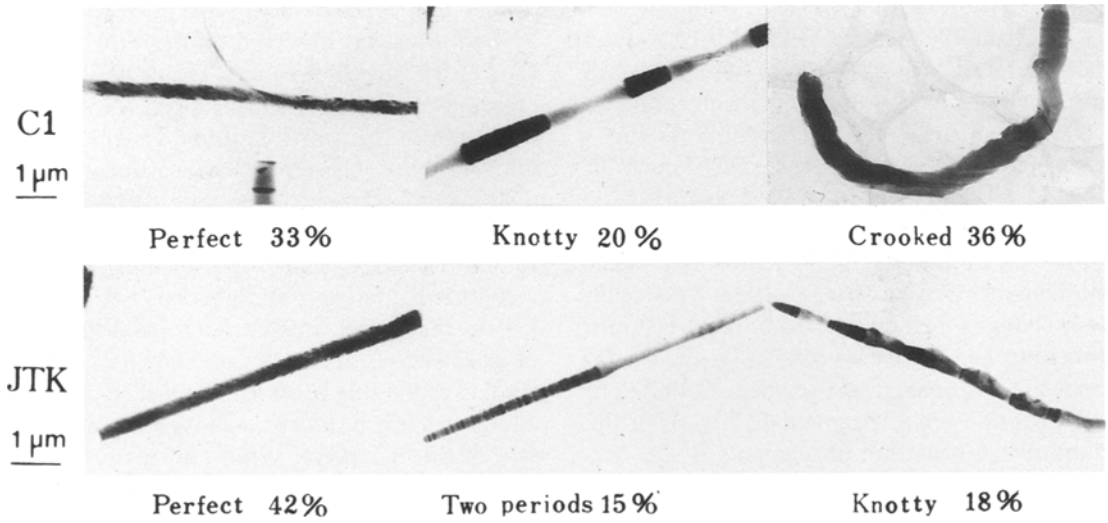

Figure 2 Variety of morphologies in the Cl and JTK SiC whiskers. Classified morphologies and the corresponding proportion of whiskers are also shown.

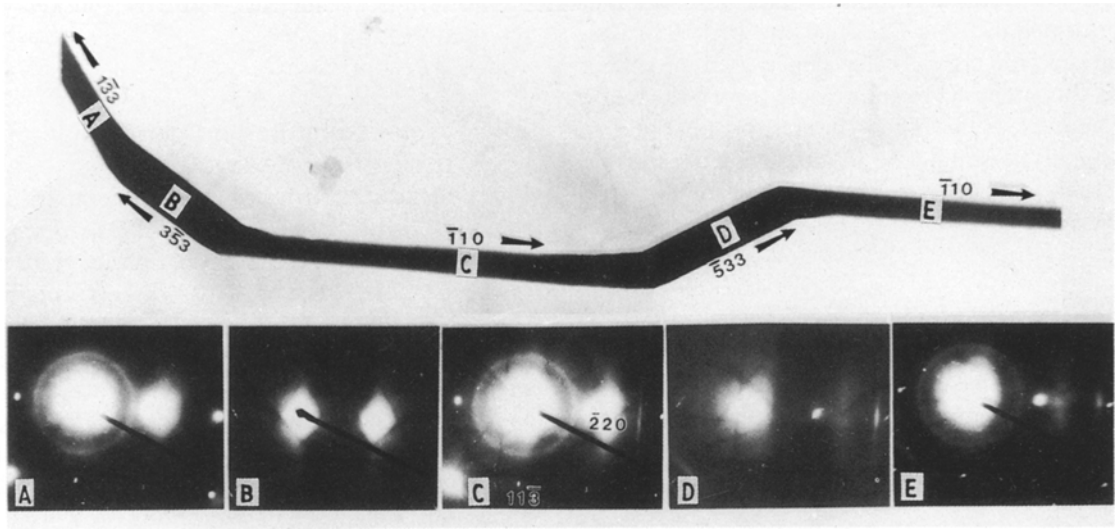

Figure 3 Contorted shape of the TiN whisker with a single-crystal structure as confirmed by electron diffraction patterns.

A more complex case appeared in the SiC whiskers. Typical morphology and the percentage of the different kinds of whisker are listed in Fig. 2 for C1 and JTK whiskers. There is only about 40% "perfect" whiskers in both SiC whiskers. Twins, planar faults and polytypes were frequently detected in electron diffraction patterns, as well as diffraction contrast micrographs.

3.2. The morphology and direction, plane of whisker growth

In addition to the straight whiskers, many tortuous TiN whiskers with a bent angle of about 145° were observed, and such zigzags may succeed over 3–5 sticks of whiskers. While the whisker changes its growth direction, its diameter may also vary. Fig. 3 shows a stick of tortuous whisker and corresponding electron diffraction patterns. All patterns coincided with the [3 3 2] zone orientation and no rotation around the electron beam was observed. This set of tortuous whiskers, in fact, is a single crystal with zigzag shape. The growth directions of the segments can be indexed as $[\bar{1}\,1\,0]$ (marked C and E in Fig. 3), $[\bar{5}\,3\,3]$ (D), $[3\,\bar{5}\,3]$ (B) and $[\bar{1}\,3\,3]$ (A). Considering that the preferential growth axes are $\langle 1\,1\,0\rangle$, $\langle 1\,1\,1\rangle$ in the TiN whiskers and the tips of whiskers were formed of octahedral $\{1\,1\,1\}$ faces [9], the peculiar morphology of the TiN whisker can be interpreted as follows. Fig. 4 shows a schematic diagram of needle whiskers with growth axes $[\bar{1}\,1\,0]$ and $[\bar{1}\,1\,1]$ and their characteristic tip shapes. If whisker growth started from segment C in Fig. 3, its $(\bar{1}\,1\,1)$ facet at the right tip became the growth basic plane of the next segment, D. As a result, the whisker changed its long axis from the $[\bar{1}\,1\,0]$ into $[\bar{1}\,1\,1]$ direction. The angle between $[\bar{1}\,1\,0]$ and $[\bar{1}\,1\,1]$ directions is 145°. Moreover, the segment D shifted to the $[\bar{1}\,1\,0]$ direction again (segment E, Fig. 3) in the opposite manner. Formation of segments B and A is similar to the case mentioned. It should be noted that the $[\bar{1}\,1\,1]$, $[1\,\bar{1}\,1]$ and $[0\,1\,1]$ directions do not lie on the (3 3 2) plane which is perpendicular to the incident electron beam. The apparent $[\bar{5}\,3\,3]$, $[3\,\bar{5}\,3]$ and $[\bar{1}\,3\,3]$ directions observed in Fig. 3, therefore, are the projected directions of the growth axes with actually low indices of the segments.

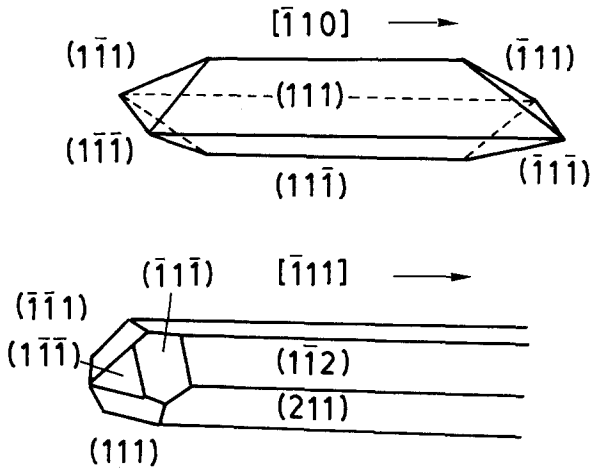

Figure 4 Schematic diagram of a TiN whisker. The tips of the needle whiskers of growth directions [1 1 0], [1 1 1] were formed of octahedral faces.

The occurrence of large-scale nucleation of secondary whiskers was observed on the TiN whiskers with the [1 0 0] growth direction. The crystallographic orientation of secondary whiskers was also in the $\langle 1\,0\,0\rangle$ direction. In this way a multiple system of perpendicular-branched whisker bushes was formed.

Most SiC whiskers have the $\langle 1\,1\,1\rangle$ growth direction; however, their outer forms are quite multitudinous. At least four types of morphology can be recognized: "perfect", straight bar; two periods stick; knotty shape and irregularly crooked lines. Two sets of whiskers, C1 and JTK, are shown in Fig. 2, where the corresponding proportions of each shape type are also given. Fig. 5 shows the cross-sections of these two sets of SiC whiskers. While the majority of the C1 whiskers are in the circular form, most JTK whiskers are hexagonal in shape. The slide thickness of the cross-section samples is about 60–70 nm. Identification of the electron diffraction pattern showed that it

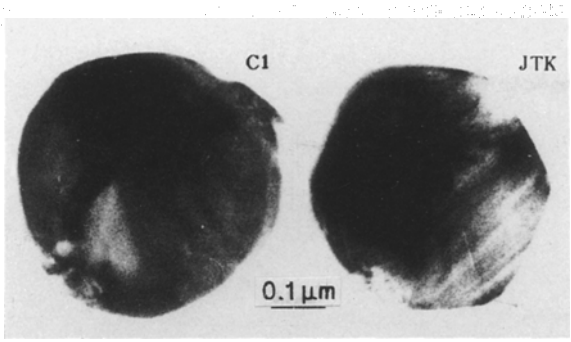

Figure 5 Whisker transverse section with (a) circular form for Cl and (b) hexagonal shape for JTK.

is hard to find β-SiC with f c c structure alone in such cross-sections, and some α-SiC with h c p structure always coexists with β-SiC. The probability of α-SiC occurring in the cross-sections is much higher than that in the dispersed samples. This fact implies that the α-SiC segment may be easier to break than the β-SiC segment, because the whisker should be broken at the weakest segment during the cutting process.

3.3. The diameter, length and ratio of L/D

The length of TiN whiskers obtained was about 10–200 μm, and the diameter varied from some tenths of a micrometre up to 2 μm. The most probable diameter was 0.8 μm, and about 41% of the whiskers could be sorted into this group. The ratio of L/D, thus, was scattered from 10–100, and the probable value should be about 60.

Fig. 6 shows the distribution of diameter and length of two sets of SiC whiskers, C1 and JTK, obtained by counting more than 700 sticks for each type of whisker. The ratio L/D was about 15–35. The diameter varied from 0.15–0.3 μm for C1, and 0.2–0.4 μm for JTK whiskers. Typical values of the diameter and length should be 0.3 and 10 μm, respectively, for both sets of whiskers.

3.4. Compositions of whisker surface and bulk

EDS analysis on TEM mode showed that chemical compositions in the whisker bulk coincided with the chemical equivalent proportion of the SiC compound, and no inclusion could be detected. Fig. 7 shows EDS spectra from the interior (Fig. 7b) and a region close to the surface of whisker C1 (Fig. 7a), where the copper peak is assumed to come from the support grid.

Because of the limited intensity of the source and the sensitivity of the detector, the surface chemical composition analysis of a single stick of whisker performed using an electron beam with spot size in the nanometre order, is very difficult at the moment. However, a combination of high-resolution images and Auger electron spectra may offer useful information about the surface state of the whiskers.

Fig. 8 shows the high-resolution image of a region close to the surface. In the [1 1 0] zone lattice image, SiC molecular columns with a separation distance of about 0.25 nm in the β-SiC structure, were well resolved. An amorphous layer with thickness about 3 nm on the surface can be clearly seen. This layer may be formed during the process of manufacturing whiskers or generated as a contamination in preparation of the specimen. From the view point of high-resolution

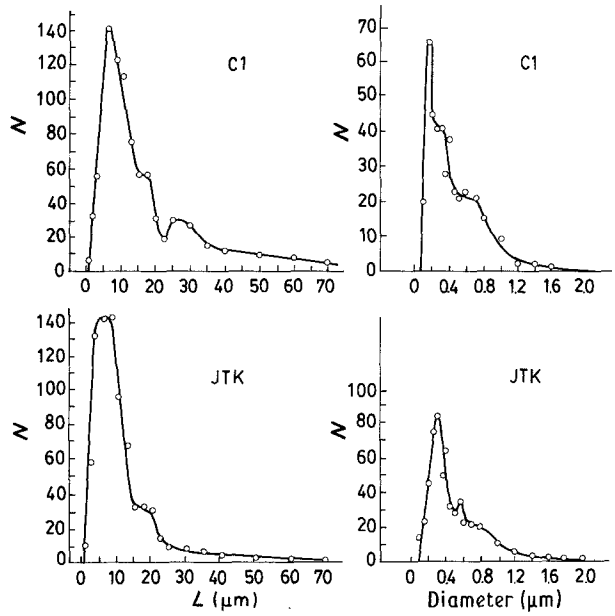

Figure 6 Length and diameter distribution of the Cl and JTK SiC whiskers.

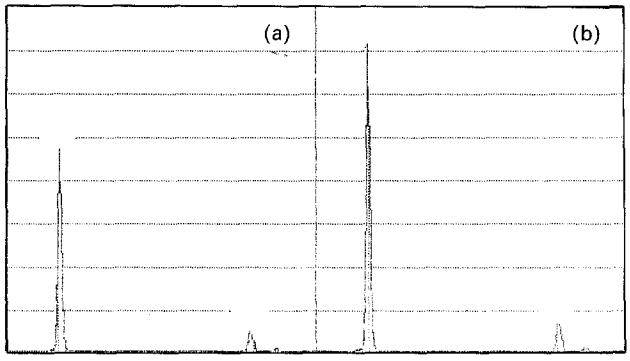

Figure 7 EDS spectrum derived from point analysis of the Cl whisker's chemistry.

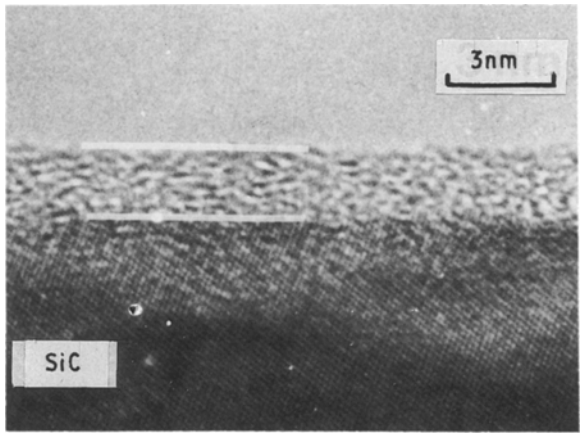

Figure 8 Surface profile image of the SiC whisker showing an amorphous layer on the SiC crystal bulk.

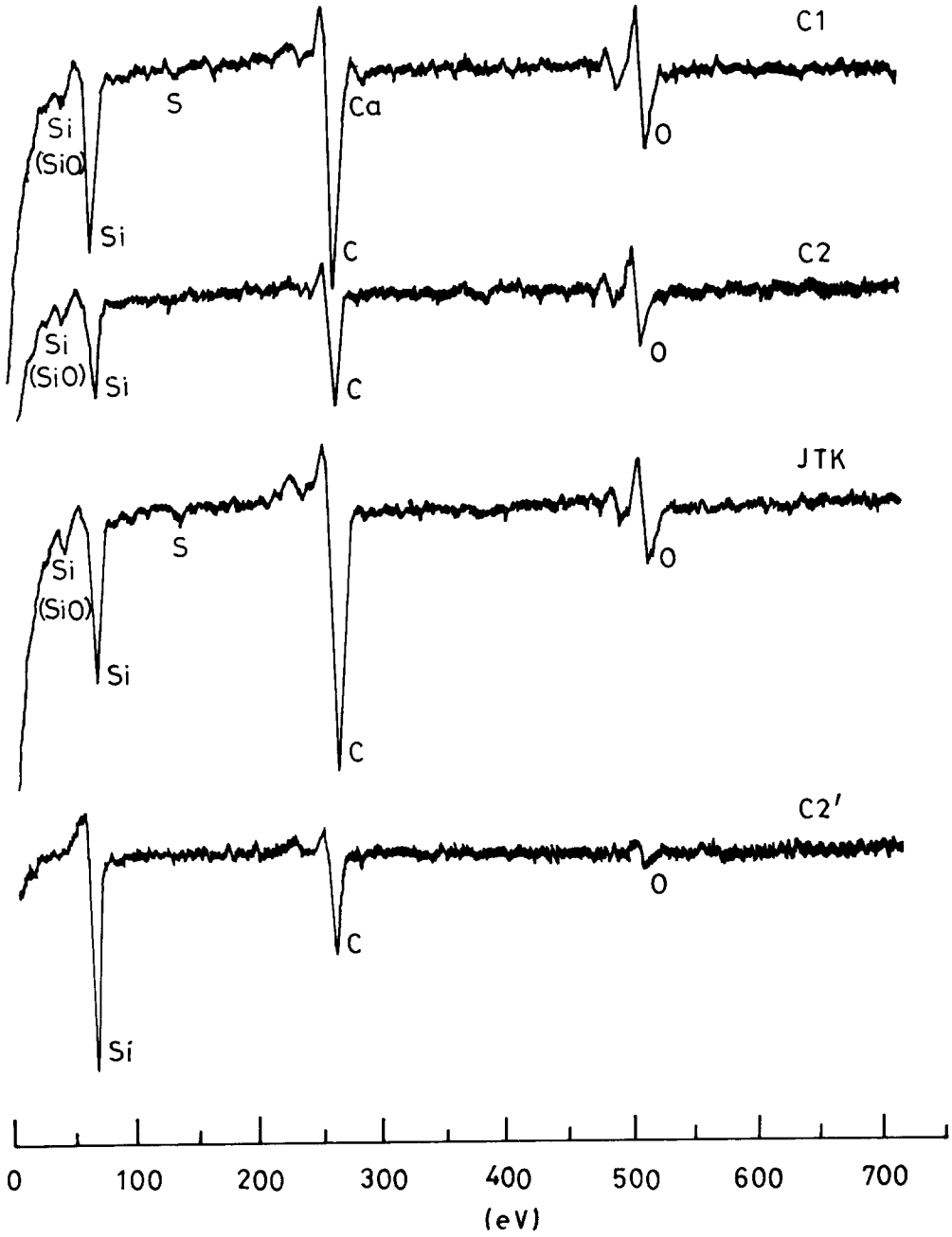

Figure 9 Auger electron spectra of the C1, C2 and JTK SiC whiskers showing their surface chemistry.

electron microscopy observations the contamination should decompose, and disappear gradually under conditions of strong electron radiation and a good vacuum in the electron microscope. In fact, this amorphous layer did not change in our observations, and seems to be an inherent part of the whisker.

The Auger electron spectrum is suitable for surface chemical analysis with a thickness of about several atomic layers, and is powerful for composition analysis of this amorphous layer. Fig. 9 gives Auger spectra of three sets of the C1, C2 and JTK whiskers, where the spectra of oxygen, sulphur and calcium at the surfaces are illustrated. As a reference, an Auger spectrum of the C1 whisker after 30 min ion peeling was also shown, and no oxygen could be detected in the interior of the SiC whiskers. The oxygen content in the surface of the C2 and JTK whiskers was in the relatively low level. The first silicon peak appeared at 86 eV, which did not correspond to the Si peak in the SiC compound (the second peak at 90 eV in Fig. 9), but referring to that in the silicate glass. It is suggested that the amorphous layer at the surface resembles SiO_2. More investigations are necessary to ascertain the influence of such an amorphous layer on the mechanical properties of composites.

3.5. Defects and their distribution

The titanium nitride obtained was quite perfect, and no defect could be detected in the diffraction contrast micrographs and high-resolution lattice images. Fig. 10 shows a [1 1 0] lattice image of the TiN whisker.

Defects in the SiC whiskers made from rice husks were identified and analysed using TEM [4, 5]. The whiskers were characterized by a high density of planar faults lying on close-packed planes perpendicular to the whisker axis. Core regions of whiskers were often filled with small inclusions ranging in size from

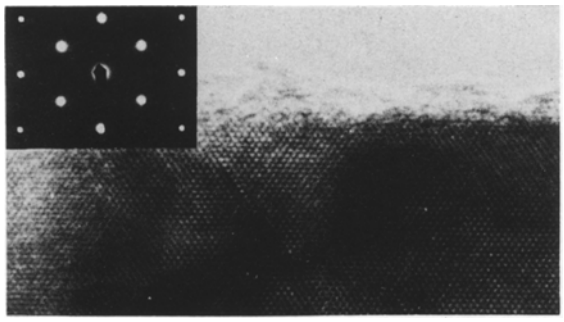

Figure 10 The [1 1 0] zone lattice image of the TiN whisker showing the perfect structure near the surface.

1–20 nm. For the present work, no inclusion could be observed in all the SiC whiskers obtained, because they were specified by very pure starting materials in their manufacture, and this coincided with the results that the surface impurity levels were low for the C2 and JTK whiskers. Two types of microtwin structure have been observed in the used SiC whiskers. One is thin lamellar twins of predominantly β-phase interspersed with stacking faults (Fig. 11). The twins are 5–20 $d_{(\bar{1}\,1\,1)}$ planar spacings wide. Within the twinned lamellae, microtwins sometimes terminated in the matrix (B in Fig. 11). Incoherent twin interfaces such as these are bounded by partial dislocations, which will be reported elsewhere shortly. The second type of microtwin structure is multiple twins, which may occur in two sets of {1 1 1} twin planes. Fig. 12 is the

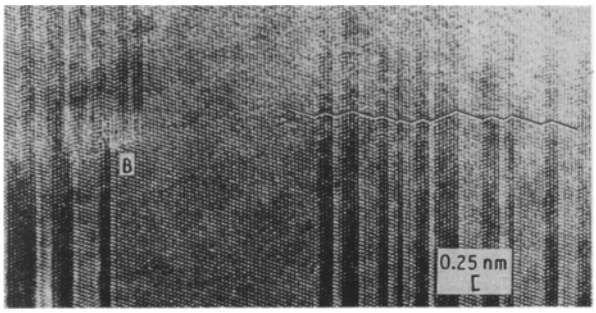

Figure 11 Irregular thin twin lamellae occurring on one family of the (1 1 1) plane shown by a high-resolution image viewed along the [1 1 0] axis.

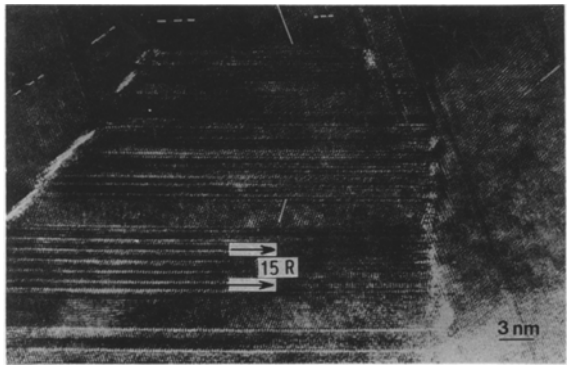

Figure 12 Multiple twins and 15R polytype structures in the SiC whisker. Projections of two sets of the {1 1 1} planes were marked by white solid and dotted lines, respectively.

[1 1 0] lattice image of the SiC whisker, where projections of the $(\bar{1}\,1\,1)$ and $(1\,\bar{1}\,1)$ planes were marked by white solid and dotted lines, respectively. Twin structures indicated by zigzag lines with mirror symmetry were easily seen. In addition to the high density of coherent twin boundaries, many incoherent twin boundaries were also seen, which seem to be the site of the coming together of a number of twins. In some cases whisker growth may be not a simple process started from a unique nucleus, but from several origins.

A number of polytypes which are variants of a one-dimensional stacking sequence of close-packed layers has been observed in chemically vapour deposited (CVD) SiC bulk and whiskers. Nutt [4] reported that several short-period polytype 9R, 4H, . . . , were identified by means of lattice fringes in the whiskers made from rice husks. However, the fringe spacing was rarely repeated more than once or twice in any location, indicating an almost random stacking sequence. Our high-resolution observation and selected-area electron diffraction could unambiguously confirm four polytypes in the SiC whiskers used, the common 3C phase (β-SiC) already shown in Figs 8 and 11, and 2H, 15R and 6H polytypes found in Figs 13, 11 and 14, respectively. It is interesting that Fig. 14 was taken from a bar of the whisker with a strange $[1\,0\,\bar{1}\,0]$ growth direction, because the normal growth axis should be [0 0 0 1] in α-SiC.

The distribution of planar defects in the SiC whiskers is similar to that reported for CVD SiC dendrites. It is known that the microstructure of CVD SiC depends strongly on the deposition temperature. Considerable planar disorder and mixtures of structural types are the characterization of the CVD SiC dendrites grown at a deposition temperature below 1400 °C. A practical concern, i.e. the probable deleterious effect of the stacking faults and polytypes on the whisker's mechanical properties, remains unknown to date. It is suggested that the techniques mentioned for investigating the microstructure of the whiskers at

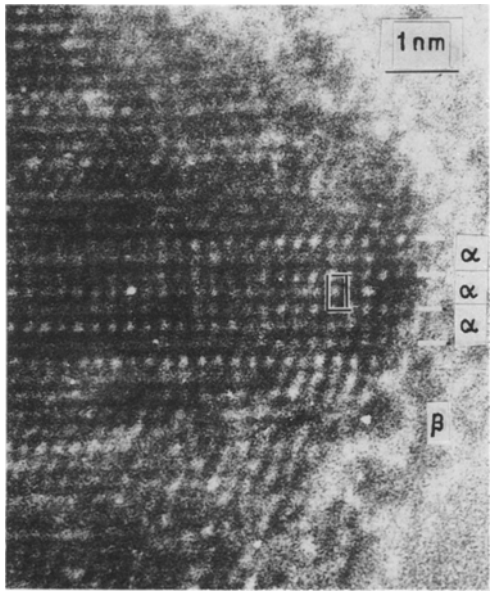

Figure 13 2H α-SiC polytype structure coexisting with β-SiC.

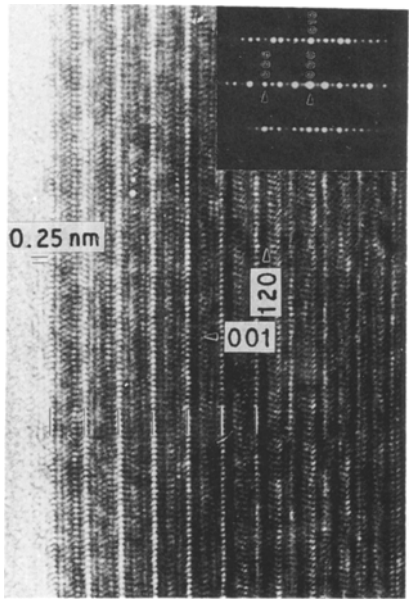

Figure 14 Electron diffraction pattern and high-resolution lattice image of 6H polytype structure in the SiC whiskers. The strange [1 0 $\bar{1}$ 0] growth direction is indicated.

high spacial resolution level could offer a powerful judgement in cases of necessity.

4. Conclusions

The microstructure of titanium nitride and silicon carbide whiskers has been evaluated according to the suggested five criteria. The main results are as follows.

1. The number of obtained SiC and TiN whiskers with single-crystal structure and a straight shape is about 50%.

2. The main growth direction is the [1 1 1] axis for both TiN and SiC whiskers. However, the [1 0 0], [1 1 0] growth axes for the TiN and the [1 0 $\bar{1}$ 0] growth direction for SiC whiskers have been observed. Crooked or perpendicular-branched whiskers were formed in the TiN whiskers. On the other hand, significant morphological variation, i.e. two periods, knotty, irregularly bent shape, etc., occur in the SiC whiskers.

3. The average length of whiskers obtained was 50 μm for TiN and 10 μm for SiC, and 0.8 μm diameter for TiN, 0.25 μm diameter for SiC, respectively. The typical ratio value of L/D varied from 60 for TiN to 25 for SiC whiskers.

4. The impurity content of the SiC whiskers used is low, probably due to starting materials with higher purity levels. The amorphous layer evinced by high-resolution imaging at the surface of the SiC whiskers resembled SiO_2 in the Auger electron spectrum. Oxygen content in the surface oxides is lower in C2, and JTK, than in the C1 whiskers.

5. The TiN whiskers are nearly perfect. There is a high density of defects in the "imperfect" SiC whiskers. For instance, stacking faults and thin twins in one or two families of {1 1 1} planes have been observed. 2H, 15R and 6H polytype structures were identified using two-dimensional lattice images.

Acknowledgements

The authors thank K. F. Zhao and Y. X. Lu, Institute of Metal Research, Chinese Academy of Sciences, Z. G. Zhu, B. Yang and Z. T. Huang, Institute of Nuclear Energy Technology, Tsinghua University, for providing the whiskers, and H. Yuan and Y. Z. Sun for the Auger spectrometer runs.

References

1. R. W. RICE, *Ceram. Engng Sci. Proc.* **2** (1981) 661.
2. Y. K. BAEK and C. H. KIM, *J. Mater. Sci.* **24** (1989) 1589.
3. R. de JONG, R. A. McCAULEY and P. TAMBUYSER, *J. Amer. Ceram. Soc.* **70** (1987) C338.
4. S. R. NUTT, *ibid.* **67** (1984) 428.
5. *Idem, ibid.* **71** (1988) 149.
6. K. R. KARASEK, S. A. BRADLEY, J. T. DONNER, M. R. MARTIN, K. L. HAYNES and H. C. YEH, *J. Mater. Sci.* **24** (1989) 1617.
7. K. F. ZHAO, C. G. BAI, W. P. HU, S. H. CHEN, X. S. FAN and F. XIA, *Mater. Sci. Progr. Sinica* **2** (1987) 52.
8. Z. T. WANG, B. Z. ZHANG, J. G. ZHU, B. YANG and S. J. XU, *ibid.* **2** (1988) 37.
9. Zb. BOJARSKI, K. WOKULSKA and Z. WOKULSKI, *J. Crystal Growth* **62** (1983) 290.

Received 23 January
and accepted 4 September 1990